Supervisory Control Implementation on Diesel-Driven Generator Sets

Knudsen, Jesper Viese; Bendtsen, Jan Dimon; Andersen, Palle; Madsen, Kjeld Kilsgaard; Sterregaard, Claes Høll

Published in:
IEEE Transactions on Industrial Electronics

DOI (link to publication from Publisher):
10.1109/TIE.2018.2811389

Publication date:
2018

Document Version
Accepted author manuscript, peer reviewed version

This article has been accepted for publication in a future issue of this journal, but has not been fully edited. Content may change prior to final publication. Citation information: DOI 10.1109/TIE.2018.2811389, IEEE Transactions on Industrial Electronics

Supervisory Control Implementation on Diesel-Driven Generator Sets

Jesper Knudsen, Jan D. Bendtsen, *Member, IEEE*, Palle Andersen, *Member, IEEE*, Kjeld K. Madsen, and Claes H. Sterregaard

***Abstract*—Diesel-driven generator sets (DGs) are widely utilized in distributed electrical power generation, due to their high reliability. This paper presents a tenth-order nonlinear state-space DG model, for which a supervisory Linear Quadratic Regulator is designed. The proposed model-based design reduces the time-consuming task of regulator tuning in comparison with current industry-standard solutions while demonstrating improved transient frequency and voltage performance, when subject to electrical load steps. These improvements are shown experimentally on two differently rated DGs.**

***Index Terms*—Diesel engines, Generators, Linear feedback control systems, Power generation control, Rapid prototyping**

I. INTRODUCTION

IN distributed electrical power generation, diesel-driven generator sets (DGs) are important components in a large range of applications, an importance only expected to increase in the coming years [1]–[3]. One vital quality of DGs is their high reliability. Typical DG applications vary from single DG solutions up to hundred-plus DG plants. Single DGs often provide, e.g., backup power at hospitals, television and radio broadcast stations, data centers, and process control facilities, whereas DG plants provide, e.g., temporary power at sporting events, musical festivals, or in remote areas [4], [5].

DG manufacturers continuously work to improve operating efficiency, including maintenance costs; however, during commissioning, that responsibility lies with the commissioning engineers and the control units they are to make use of. Unfortunately, human involvement may often lead to suboptimal and/or inconsistent tuning and performance.

In many applications, DGs are equipped with a supervisory control unit, denoted the Automatic Genset Controller (AGC), adding capabilities such as synchronization, active and reactive power control, and automatic mains failure response. As shown in Fig. 1, two primary controllers are always present; the governor for engine control and the Automatic Voltage Regulator (AVR) for generator control [6]. The global market-leading manufacturers of AGC units all implement fundamentally equivalent regulation algorithms, based on classical proportional-integral-derivative (PID) regulators. Through many years of industrial use the PID regulator has proven its worth in terms of simplicity and reliability. A PID regulator is simple to implement, as it requires limited system information, and simple to adjust due to the straightforward interpretation of the regulation parameters. However simple, regulation parameter adjustments must be performed for each DG; a time-consuming task, which is critical to the performance.

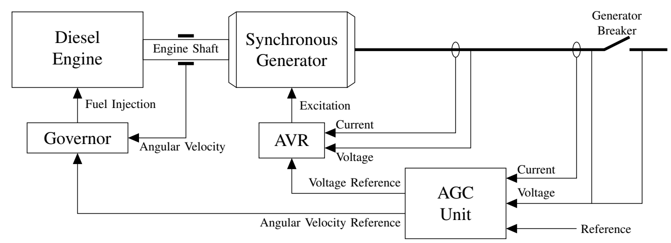

Fig. 1. DG control system with the fuel injection regulating governor, the excitation regulating AVR, and the supervisory AGC unit.

Implementing a regulator that can reduce, or possibly remove, the need for time-consuming manual adjustments while keeping the commissioning engineering interface simple, could aid in improving DG efficiency in terms of commissioning costs and possibly operational efficiency through automated adjustment procedures.

Control of diesel-driven generator sets, in various applications, has been presented in works such as [7]–[21]. However, the vast majority concerns control design for governor and/or AVR, individually or in combination. To the best of the authors' knowledge, only [20] presents work that relates directly to AGC design. However, applying constant-gain PI regulation as [20] on complex and highly nonlinear systems, such as DGs, will in many cases yield suboptimal performance.

In the present work, AGC regulator design for frequency and voltage stabilization of an islanded DG exposed to load changes is considered. Demonstrating implementation results of an AGC design on two differently rated DGs, this paper extends and enhances the work in [22], [23]. The implemented AGC design utilizes Linear Quadratic Regulator (LQR) feedback of estimated system states for a tenth-order nonlinear control-oriented first principles-based state-space DG model. Certain model parameter values can be derived directly from

Manuscript received December 1, 2017; revised January 24, 2018; accepted February 13, 2018. This work was supported by Innovation Fund Denmark and DEIF as part of a Danish Industrial Ph.D. Project [Application Number 4135-00108B].

J. Knudsen, K. K. Madsen, and C. H. Sterregaard are with the Power & Marine Division, DEIF, 7800 Skive, Denmark (e-mail: jek@deif.com; kma@deif.com; chn@deif.com).

J. D. Bendtsen and P. Andersen are with the Section for Automation and Control, Department of Electronic Systems, Aalborg University, 9220 Aalborg, Denmark (e-mail: dimon@es.aau.dk; pa@es.aau.dk).

This article has been accepted for publication in a future issue of this journal, but has not been fully edited. Content may change prior to final publication. Citation information: DOI 10.1109/TIE.2018.2811389, IEEE Transactions on Industrial Electronics

engine and generator datasheets, whereas others must be identified from measurement data. The model complexity is sufficient to describe the dynamical behavior of actual DGs, while remaining suitable for control design; as demonstrated by experimental results. The structure of LQRs enables incorporation of well-known cross dependencies between frequency and voltage, and generally exploiting system knowledge, in the control design, which is not common practice in PID implementations. Additionally, designing the control system for a set of operating points improves the ability to handle varying system dynamics throughout the operating range.

The remainder of the paper is organized as follows. Section II presents the DG model while Section III provides the AGC regulator design, which builds on the design presented in [23]. Section IV introduces the utilized experimental setup while Section V presents the experimental results. Finally, Section VI provides concluding remarks.

II. Diesel-Driven Generator Set Model

The explicit time dependency of variables is suppressed throughout the paper. Note that all variables, constants, etc., are assumed scalar and real unless stated otherwise.

A. Diesel Engine and Governor

In preparation for a generic LQR control design, the diesel engine model utilizes per unit values, in agreement with the synchronous generator model, such that all states of the model evolve within the same range. This entails utilizing a per unit swing equation to describe the rotary behavior of the synchronous machine given by

$$J\underline{\omega}_m\dot{\omega}_m = \underline{T}_m T_m - \underline{T}_e T_e - D\underline{\omega}_m\omega_m \tag{1}$$

where ω_m is the per unit angular velocity of the shaft, T_m and T_e are the per unit mechanical and electrical torques applied to the shaft, J and D are the total system inertia and damping, and $\underline{\omega}_m$, $\underline{T}_m$ and $\underline{T}_e$ are the mechanical angular velocity base, mechanical torque base, and electrical torque base, respectively. For clarity, these base values denote the nominal angular velocity of the crankshaft, the rated engine torque at rated angular velocity, and the rated electrical torque at rated voltage and frequency, respectively. Additionally, the dynamics of the per unit mechanical torque T_m delivered to the shaft by the diesel engine are given by

$$\dot{T}_m = \frac{1}{\tau_m(1+T_m)}(\mu - T_m) \tag{2}$$

where τ_m is the constant term of the engine time constant and μ is the per unit fuel injection requested by the governor. This first-order differential equation with a varying time constant is introduced to accommodate observations of increased retarding from the time between load impact to mechanical torque changes at increased torque levels.

A governor is included in the DG model as a PI regulator attempting to maintain nominal per unit angular velocity of the shaft ω_m; a control scheme referred to as isochronous mode. The governor control law is given by

$$\dot{e}_{i\omega} = r_\omega + u_\omega - \omega_m \tag{3a}$$

$$\mu = k_{p\omega}(r_\omega + u_\omega - \omega_m) + k_{i\omega}e_{i\omega} \tag{3b}$$

where $e_{i\omega}$ is the governor integral error state, r_ω is the per unit angular velocity internal governor reference, which in isochronous mode remains at nominal value, u_ω is the per unit angular velocity reference offset, which is one control variable of the supervisory AGC, and $k_{p\omega}$ and $k_{i\omega}$ are the proportional and integral governor regulator gains.

B. Synchronous Generator and AVR

The synchronous generator model is expressed in per unit dq-components [24], with subscripts indicating the specific dq-component. The per unit flux linkages ψ and their associated per unit time derivatives $\dot{\psi}$ are given by [6]

$$\psi_d = -L_d i_d + L_{ad} i_f + L_{ad} i_{1d}, \quad \dot{\psi}_d = v_d + \psi_q\omega_e + R_a i_d \tag{4a}$$

$$\psi_q = -L_q i_q + L_{aq} i_{1q}, \quad \dot{\psi}_q = v_q - \psi_d\omega_e + R_a i_q \tag{4b}$$

$$\psi_f = L_{ff} i_f + L_{f1d} i_{1d} - L_{ad} i_d, \quad \dot{\psi}_f = v_f - R_f i_f \tag{4c}$$

$$\psi_{1d} = L_{11d} i_{1d} + L_{f1d} i_f - L_{ad} i_d, \quad \dot{\psi}_{1d} = -R_{1d} i_{1d} \tag{4d}$$

$$\psi_{1q} = L_{11q} i_{1q} - L_{aq} i_q, \quad \dot{\psi}_{1q} = -R_{1q} i_{1q} \tag{4e}$$

where i's are per unit generator currents, L's are per unit self and mutual inductances, R's are per unit resistances, ω_e is the per unit electrical angular velocity, which is assumed equal to ω_m, v_d and v_q are per unit terminal voltages, and v_f is the per unit field excitation voltage set by the AVR. The control law of the included AVR, modeled as a PI regulator, attempting to maintain nominal per unit three-phase phase-to-neutral RMS voltage v_{rms} is given by

$$\dot{e}_{iv} = r_v + u_v - v_{rms} \tag{5a}$$

$$v_f = k_{pv}(r_v + u_v - v_{rms}) + k_{iv}e_{iv} \tag{5b}$$

where e_{iv} is the AVR integral error state, r_v is the per unit three-phase phase-to-neutral RMS internal AVR voltage reference, which in isochronous mode remains at nominal value, u_v is the per unit three-phase phase-to-neutral RMS voltage offset, which is the second control variable of the supervisory AGC, and k_{pv} and k_{iv} are the proportional and integral AVR regulator gains. Calculating RMS values are in practice based on measurements of the latest full period of the alternating signal. For balanced systems, this effectively amounts to a filtering of an instantaneous RMS value. This filtering is approximated as a first-order low-pass filter, providing

$$\dot{v}_{rms} = \frac{1}{\tau_v}\sqrt{\frac{1}{2}\left(v_d^2 + v_q^2\right)} - \frac{1}{\tau_v}v_{rms} \tag{6}$$

where τ_v is the filter time constant of twice the per unit time period of the nominal frequency.

C. Electrical Load

The dynamics of an islanded DG are significantly impacted by the connected electrical load. In preparation for applying LQR, the electrical load is modeled as a pure resistance. This simplifying choice aligns with the possibilities in the available

This article has been accepted for publication in a future issue of this journal, but has not been fully edited. Content may change prior to final publication. Citation information: DOI 10.1109/TIE.2018.2811389, IEEE Transactions on Industrial Electronics

experimental setup, which is described in Section IV, and is challenged to the extent possible in Section V. The terminal voltages are then given by

$$\begin{bmatrix} v_d \\ v_q \end{bmatrix} = R_L \Lambda \begin{bmatrix} \psi_d & \psi_q & \psi_f & \psi_{1d} & \psi_{1q} \end{bmatrix}^T \tag{7}$$

where R_L is the per unit per phase load resistance and the non-zero elements of $\Lambda \in \mathbb{R}^{2\times 5}$ contain inductances [6].

D. Complete State-Space Model

Putting the above together, a tenth-order nonlinear state-space model on the form

$$\dot{x} = A(x_2)x + B_1 w + B_2 \sqrt{\frac{1}{2}(w_1^2 + w_2^2)} + B_3(x_2)(r+u) + x_1 F_1 x + x_3 F_3 x + x_4 F_4 x \tag{8a}$$

$$y = Cx \tag{8b}$$

is obtained, where x, w, r, u, and y are the state, terminal voltage, internal reference, supervisory control variable, and output vectors, respectively, given by

$$x = \begin{bmatrix} \omega_m & T_m & \psi_d & \psi_q & \psi_f & \psi_{1d} & \psi_{1q} & e_{i\omega} & e_{iv} & v_{rms} \end{bmatrix}^T \tag{9a}$$

$$w = \begin{bmatrix} v_d & v_q \end{bmatrix}^T, \quad r = \begin{bmatrix} r_\omega & r_v \end{bmatrix}^T \tag{9b}$$

$$u = \begin{bmatrix} u_\omega & u_v \end{bmatrix}^T, \quad y = \begin{bmatrix} \omega_m & v_{rms} \end{bmatrix}^T \tag{9c}$$

and the matrices $A(x_2) \in \mathbb{R}^{10\times 10}$, $B_1 \in \mathbb{R}^{10\times 2}$, $B_2 \in \mathbb{R}^{10\times 1}$, $B_3(x_2) \in \mathbb{R}^{10\times 2}$, $C \in \mathbb{R}^{2\times 10}$, $F_1 \in \mathbb{R}^{10\times 10}$, $F_3 \in \mathbb{R}^{10\times 10}$, and $F_4 \in \mathbb{R}^{10\times 10}$ follow from the introduced relations.

Datasheet values are utilized for parameters concerning the system inertia, the torque bases, the armature resistance of the generator stator, and the self and mutual stator inductances. Alternatively, the system damping is determined in accordance with [22], while the generator rotor parameters are chosen to match the per unit values of the 'Synchronous Machine Salient Pole (fundamental)' block [25] from the Simscape Power Systems toolbox of MATLAB Simulink®, which are based on models described in [6], [26]. In general, parameters related to the rotor cannot be assumed available, since the standards applicable to the test procedures relevant for determining datasheet content do not include methods for determining all those parameters [27], [28]. Datasheets [29], [30] represent typical datasheets with the amount of content that can be assumed available. Finally, τ_m, $k_{p\omega}$, $k_{i\omega}$, k_{pv}, and k_{iv} must be found based on system measurements using a parameter identification method. In the present work, the parameters were determined without much effort through trail and error; however, a more sophisticated approach would be beneficial for future implementations. All model parameters utilized to obtain the experimental results are provided in Table I.

III. Automatic Genset Controller Design

The LQR method is chosen due to is generic design nature, which can provide a simple regulator tuning interface. Applying the traditional LQR method requires a linear model of the system and internal state information, which is not immediately measurable in typical DG systems. Thus, model linearization and state estimation is required before such a regulation scheme can be employed.

TABLE I
Model parameter sets for both DGs utilized.

Parameter	Unit	Diesel Generator 1	Diesel Generator 2
J	kg·m^2	1.8015	2.1654
D	N·m·s/rad	0.1	0.1
$\underline{\omega}_m$	rad/s	50π	50π
$\underline{T}_m$	N·m	390	265
$\underline{T}_e$	N·m	381.97	254.65
τ_m	s	0.1	0.075
$k_{p\omega}$	-	8	13
$k_{i\omega}$	-	15	31
L_d	p.u.	2.83	1.9
L_q	p.u.	1.69	0.98
L_{ad}	p.u.	2.38	1.6
L_{aq}	p.u.	1.24	0.68
L_l	p.u.	0.45	0.3
R_a	p.u.	0.0354	0.0208
L_{ffd}	p.u.	2.6371	1.8571
L_{11d}	p.u.	2.58	1.8
L_{11q}	p.u.	1.4967	0.9367
L_{f1d}	p.u.	2.38	1.6
R_f	p.u.	0.0006	0.0006
R_{1d}	p.u.	0.0354	0.0354
R_{1q}	p.u.	0.0428	0.0428
k_{pv}	-	0.03	0.011
k_{iv}	-	0.06	0.009
τ_v	p.u.	0.0064	0.0064

A. Model Linearization

The nonlinear DG model is linearized using first-order Taylor series expansion, treating R_L as a disturbance input rather than v_d and v_q, following the relation given by (7). Additionally, R_L is chosen as the variable that determines the active operating point; its value is found utilizing voltage and current measurements and will therefore at all times equal the true load resistance (within measurement accuracies) assuming a balanced three-phase load. The set of operating points is selected for a specific DG as detailed in Section V. Derivations of the linear models are presented in [23].

B. Large-Signal State Estimation

In an effort to circumvent potential issues related to state discontinuities of classical Luenberger small-signal state estimators [31], a large-signal state estimator, as formulated in [23], is utilized. In the present work, the operating point values of the control variables u are at all times zero, because they represent offsets. The large-signal state estimator is given by

$$\dot{\hat{x}} = \bar{A}_i \hat{x} + \bar{B}_i u + \bar{B}_{di} \hat{d} + L_i \big(y - \bar{C}_i \hat{x}\big) - \bar{A}_i \bar{x}_i - \bar{B}_{di} \bar{d}_i \tag{10}$$

where $\hat{x}$ is the estimated large-signal per unit states, $\hat{d}$ is the estimated electrical load given by the calculated R_L, $\hat{y}$ is the estimated large-signal per unit output, L_i is the estimator gain matrix of the i-th operating point, $\bar{x}_i$ and $\bar{d}_i$ are the operating point values of the estimated states and electrical load for the i-th operating point, matrices $\bar{A}_i \in \mathbb{R}^{10\times 10}$, $\bar{B}_i \in \mathbb{R}^{10\times 2}$, $\bar{B}_{di} \in \mathbb{R}^{10\times 1}$, and $\bar{C}_i \in \mathbb{R}^{2\times 10}$ are the linearized system matrices of the i-th operating point, found according to the procedure shown in [23], and $i \in \{1, \ldots, n_{op}\}$ where n_{op} is the number of operating points for the specific DG.

This article has been accepted for publication in a future issue of this journal, but has not been fully edited. Content may change prior to final publication. Citation information: DOI 10.1109/TIE.2018.2811389, IEEE Transactions on Industrial Electronics

C. Linear Quadratic Regulator

The theory of LQR state feedback is thoroughly described in literature and will, due to space considerations, not be presented here; instead, the reader is referred to [32], [33] for details. The AGC control law with state feedback of the large-signal estimated states $\hat{x}$ through the LQR state feedback matrix K_i of the i-th operating point is given by

$$u = -K_i\hat{x} + K_i\bar{x}_i, \qquad i \in \{1, \dots, n_{op}\} \tag{11}$$

where the second term is included to accommodate the use of a large-signal state estimator.

The complete closed-loop AGC regulator design is shown in Fig. 2, where d is electrical load connected to the DG. Switching of i is implemented unfiltered; that is, without guarantees on, e.g., average dwell-time [34], which is very likely to be relevant in other implementations.

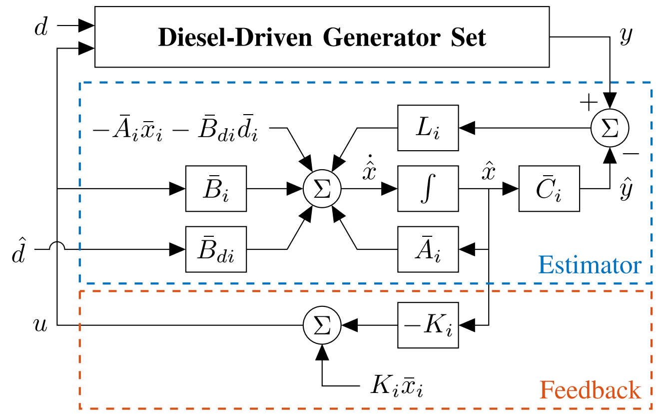

Fig. 2. Closed-loop AGC regulator design diagram, including large-signal state estimator and LQR state feedback. Note, all operating point discontinuities have been moved in front of the integration by the reformulation to a large-signal state estimator.

IV. Experimental Setup

In this section, the physical setup used for model validation and to obtain the following implementation results is presented in detail. Fig. 3 shows the test room at the headquarters of DEIF in Skive, Denmark in which the experimental setup is located. The relevant elements and their interconnections are shown in Fig. 4 as a single-line diagram. Denoted DG 1, a 60 kVA DG, connects through Generator Breaker 1 to the load bank at the busbar. Denoted DG 2, a 40 kVA DG, similarly, connects through Generator Breaker 2 to the load bank at the busbar. As the proposed regulator does not include synchronization and load-sharing capabilities, the two generator breakers are never closed at the same time while the proposed regulator is active. The DGs are rated at a power factor of 0.8, which is typical in this industry.

DG 1 is made up of a turbocharged, four-stroke, four-cylinder Deutz BF4M2012 diesel engine and a salient four-pole, three-phase, brushless, synchronous, 60 kVA/48 kW at 50 Hz Leroy-Somer LSA 42.3 L9 C6/4 generator. The engine is controlled by a Deutz EMR 2 governor and the generator is controlled by a DEIF DVC310 AVR, with both the governor and the AVR set to run in isochronous regulation mode.

DG 2 consists of a turbocharged, four-stroke, four-cylinder Deutz BF4M1011F diesel engine and a salient four-pole, three-phase, brushless, synchronous, 40 kVA/32 kW at 50 Hz Mecc Alte Spa ECO 32-3S/4 generator. The engine is controlled by a Huegli Tech HT-SG-100 governor while the generator is controlled by a DEIF DVC310 AVR; both operating in isochronous regulation mode.

The load bank is a system of active and reactive load elements, which can be connected in parallel. The load elements enable an applied active load from 0 to 100 kW in steps of 10 kW and reactive load from 0 to 50 kVAr in steps of 5 kVAr.

The proposed AGC regulator design is applied to the DG through a Rapid Control Prototyping (RCP) system based on a dSPACE DS1103-07 400 MHz PPC controller board [35]. The system has access to the frequency, which is obtained through a magnetic pick-up on the engine shaft, and all the three phase voltages and currents. The RCP is executed at a 10 kHz base frequency with measurement intervals determined by the rotational speed of the engine shaft to provide 16 samples per period. The control signal from the proposed regulator to the governor and AVR is sent as a 40 ms Controller Area Network (CAN) J1939 message, resembling a typical communication speed and protocol of industrial AGC units.

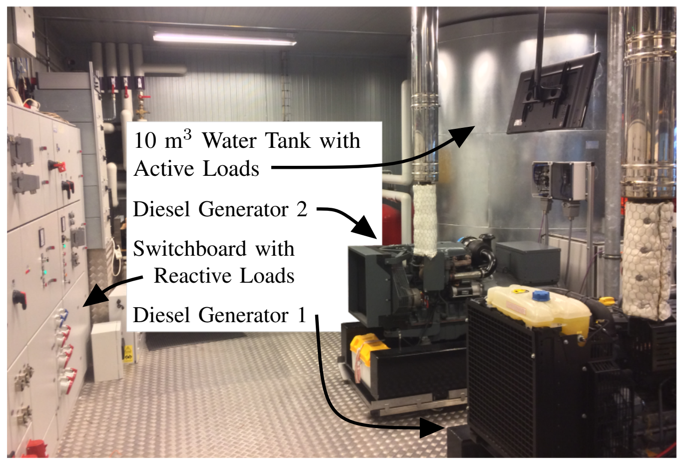

Fig. 3. Test room at the headquarters of DEIF in Skive, Denmark.

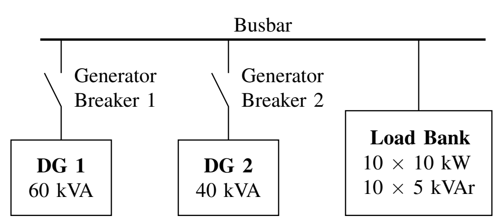

Fig. 4. Single-line diagram of the laboratory facilities, consisting of two diesel-driven generator sets connected through individual generator breakers to the load bank at the busbar.

Measurements presented in Section V are collected using a HIOKI Memory HiCorder 8861 with High Resolution Unit 8957 input modules. All measurements from the HIOKI data collection system are taken at a 50 kHz sampling rate.

This article has been accepted for publication in a future issue of this journal, but has not been fully edited. Content may change prior to final publication. Citation information: DOI 10.1109/TIE.2018.2811389, IEEE Transactions on Industrial Electronics

V. Experimental Results

This section presents experimental results obtained implementing the proposed AGC LQR design by use of the RCP system; both on DG 1 and DG 2, in separate experiments, to demonstrate the applicability of the design.

As DG 1 and DG 2 are given by different sets of model parameters, unique regulator and estimator gains have been calculated for every operating point of each DG. However, all those gains have been calculated using similar tuning parameter values. That is, the LQR feedback gain matrices K_i for all operating points i have been found by applying the diagonal weighting matrices

$$Q = \mathrm{diag}\big(\begin{bmatrix}25 & 1 & 1 & 1 & 1 & 1 & 1 & 1 & 1 & 1\end{bmatrix}\big) \tag{12a}$$
$$R = \rho I_{2\times 2} \tag{12b}$$

where ρ is a scalar regulator tuning knob, analyzed in the following. Equations (12) penalize deviations in the per unit mechanical angular velocity ω_m and, for $\rho > 1$, the two inputs higher than deviations in the remaining states. Further, calculation of the large-signal state estimator gain matrices L_i for all operating points i for both DGs has been done identically. That is, the poles of each $\bar{A}_i - L_i\bar{C}_i$ are placed at the values given by the multiplication of the pole values of the corresponding $\bar{A}_i - \bar{B}_i K_i$ by three. This is done using MATLAB's implementation of the robust pole assignment algorithm presented in [36], i.e., the function `place()`.

The operating point sets for DG 1 and DG 2 are chosen to coincide with the available resistive load elements, accommodating the rating of each DG. That is, the operating points for DG 1 are 10, 20, 30, 40, and 50 kW, while for DG 2 the operating points are 10, 20, and 30 kW.

The frequency and voltage transients in response to steps in active load are shown in Figs. 5 and 6 for DG 1 with $\rho = 200$. In these figures, measurements of an open-loop implementation, i.e., constant nominal references with no offset for the governor and AVR, and of an industry-standard PID regulator AGC implementation is provided for comparison. The PID regulator has been tuned by an independent commissioning engineer, in order to achieve realistic industry performance. The transient dynamics are inherently restricted by the engine in particular, but also the generator. Hence, striking transient improvements should not be expected since the governor and AVR of the open-loop implementation are already optimized by the manufacturers to deal with this scenario.

In general, an improvement in transient response on the open-loop implementation is observed for the LQR implementation in both frequency and voltage on DG 1 with less overshoot and shorter settling times. Note that the PID implementation, according to most performance criteria, delivers worse transient responses than both the LQR and the open-loop implementations. However, the integral action of the PID regulator means the PID implementation is the only implementation able to sustain nominal frequency and voltage in any feasible steady-state condition; implying that the integral action of the governor and AVR is, in practice, insufficient.

The main objective of the proposed supervisory controller is to reduce tuning complexity. As demonstrated in Figs. 7 and 8, this is accomplished through one intuitive tuning handle; the parameter ρ in (12b). Alterations of R entail different deviation penalties on the inputs, which lead to increased or reduced regulator activity. Utilizing $\rho = 100$ yields a more aggressive regulation, referred to as Fast LQR in Figs. 7 and 8. Using $\rho = 200$ obtains the regulation performance presented previously in Figs. 5 and 6, now referred to as Mild LQR. Finally, $\rho = 300$ yields the regulation referred to as Slow LQR in Figs. 7 and 8, which in general approaches the regulation performance of the open-loop implementation. Although demonstrated here only on DG 1, due to space considerations, the procedure has been applied equally successfully on DG 2 using a similar range of

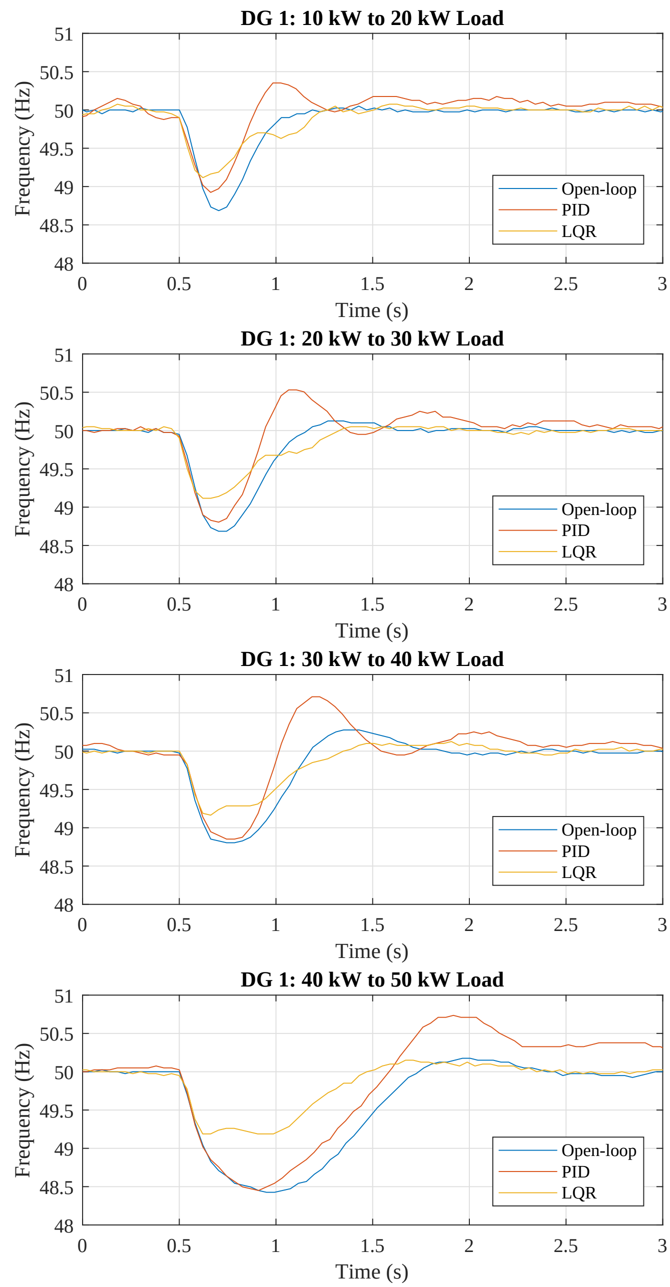

Fig. 5. Frequency transients following steps in active load with industry-standard PID, the proposed LQR, and no supervisory controller on the 60 kVA DG 1 with isochronous governor and AVR.

This article has been accepted for publication in a future issue of this journal, but has not been fully edited. Content may change prior to final publication. Citation information: DOI 10.1109/TIE.2018.2811389, IEEE Transactions on Industrial Electronics

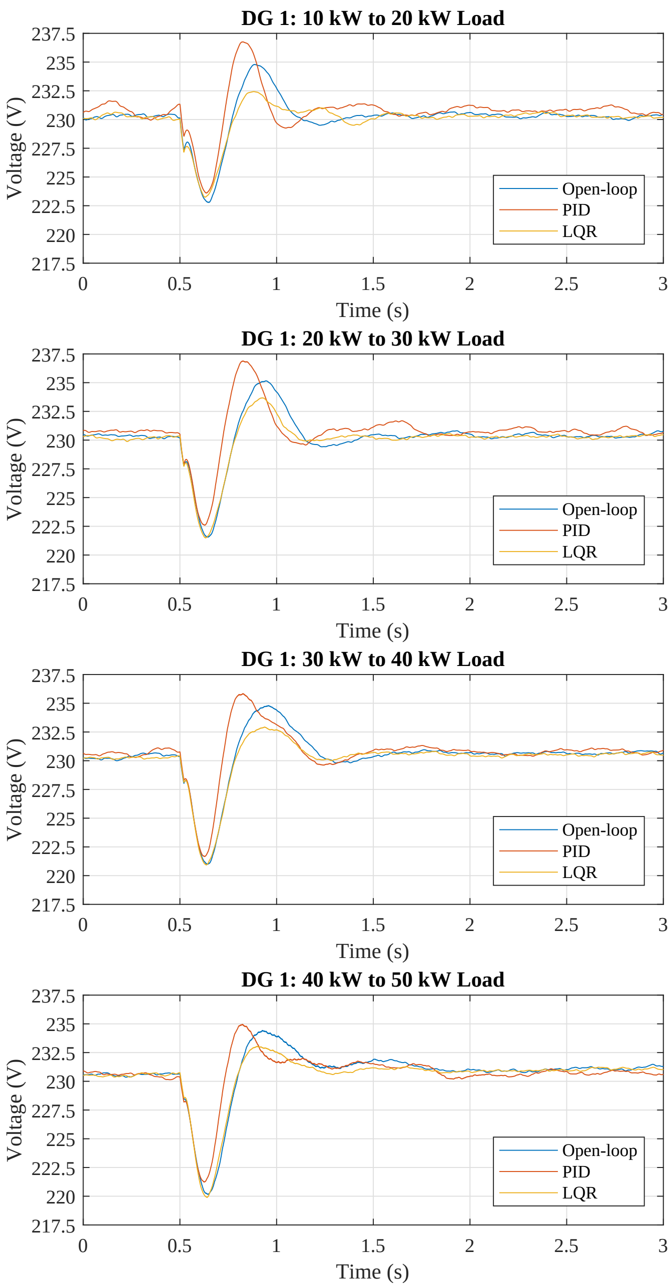

Fig. 6. Voltage transients following steps in active load with industry-standard PID, the proposed LQR, and no supervisory controller on the 60 kVA DG 1 with isochronous governor and AVR.

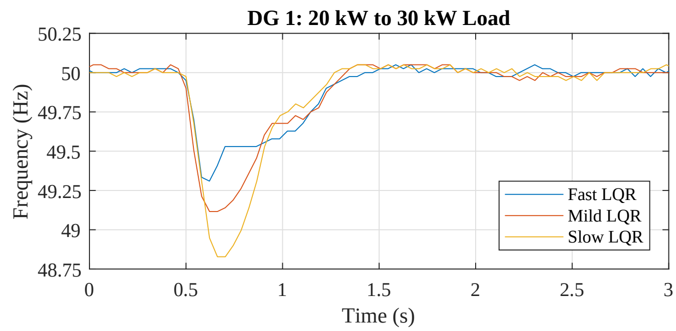

Fig. 7. Frequency transients following steps in active load using the proposed supervisory LQR design with Fast ($\rho = 100$), Mild ($\rho = 200$), and Slow ($\rho = 300$) tuning on the 60 kVA DG 1.

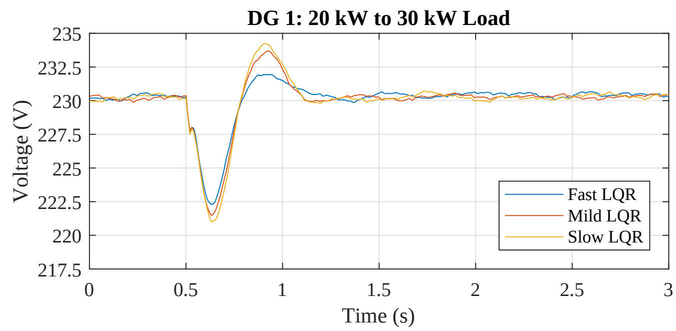

Fig. 8. Voltage transients following steps in active load using the proposed supervisory LQR design with Fast ($\rho = 100$), Mild ($\rho = 200$), and Slow ($\rho = 300$) tuning on the 60 kVA DG 1.

variation for ρ in the regulator design.

As a part of the modeling and linearization approach presented in Sections II-C and III-A, the effects of any non-resistive electrical load elements has been neglected. In an effort to challenge this approach, DG 2 has also been exposed to steps in apparent power, i.e., simultaneous steps in active and reactive load. Figs. 9 and 10 present the obtained frequency and voltage transients with the same LQR implementation for steps in load of active power and apparent power. The extraordinary initial drop in voltage for steps in apparent power is similar to the drops obtained with the industry-standard PID and open-loop implementations. These results clearly demonstrate the applicability of the proposed supervisory controller on differently rated DGs and during alternative load conditions not included in the model.

The final remarks on the results concern the complexity of DGs. The nature of DG 2, with all its components, is one that dictates a rather conservative regulation, something even a highly experienced commissioning engineer cannot know a priori, whereas DG 1 is more lenient towards aggressive regulation. Such observations encourage a self-tuning scheme that sets off from a conservative starting point. Lastly, comparing the open-loop measurements of Figs. 5 and 6 with the open-loop measurements presented from DG 1 in [22], a significant difference in the time it takes to return to nominal frequency following the step from 40 kW to 50 kW is noted. Possibly owing to general engine wear and tear, such variations in dynamic behavior occur frequently in real-life systems and must be anticipated. The current approach, evidently, has a certain robustness against this degree of parameter variation, since no adjustments were made to accommodate it. That is, the parameter identification was completed using the measurements in [22], while for the control design experiments presented here, which were carried out at a later point in time, the system exhibits different dynamics.

VI. Conclusion

The model-based supervisory AGC design developed and experimentally demonstrated in this paper, shows promising features in terms of achieving improvements to the current

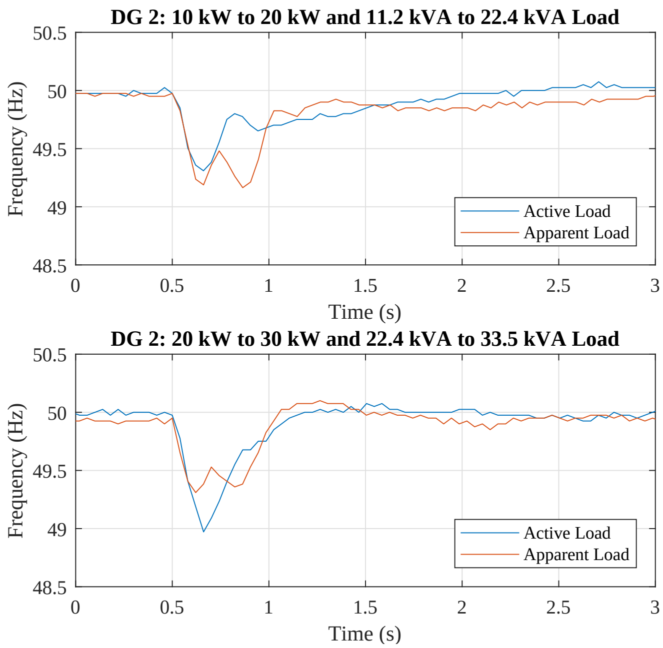

Fig. 9. Frequency transients following steps in active or apparent load with the proposed supervisory LQR on the 40 kVA DG 2 with isochronous governor and AVR.

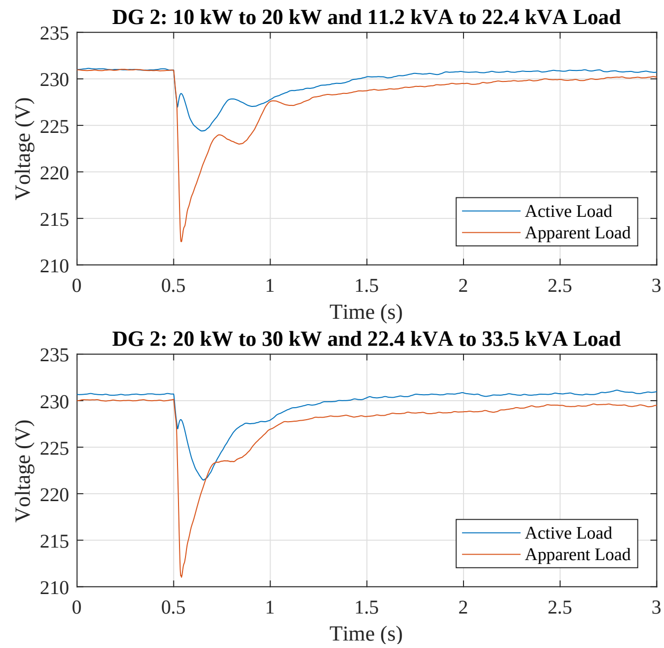

Fig. 10. Voltage transients following steps in active or apparent load with the proposed supervisory LQR on the 40 kVA DG 2 with isochronous governor and AVR.

industry-standard solutions. As shown in Section V, replacing the current PID-based design with an LQR-based design can offer a simpler regulator tuning interface for commissioning engineers in addition to obtaining improved transient performance following changes of supplied electrical load.

Through the generic nature of the model and control design, the proposed supervisory control approach facilitates a self-tuning implementation; thus, designing a reliable automated parameter identification method would be a natural next step in any future development. Additional future work could include an investigation of, e.g., feedback linearization or genuine nonlinear control algorithms, in an attempt to remove the need for operating point specifications and calculations.

REFERENCES

[1] G. Johnson, "Generator Sets Report," IHS Technology, Tech. Rep., 2014.
[2] G. Johnson, "Short-term headwinds, long-term growth for generator sets market," 2016. [Online]. Available: https://technology.ihs.com/582961/short-term-headwinds-long-term-growth-for-generator-sets-market
[3] Mordor Intelligence, "Global Diesel Generator Market - Analysis by Deployment Location - Growth Trends and Forecasts (2016 - 2021)," Tech. Rep., 2016.
[4] DEIF, *Land Power Application Guide*, 2016.
[5] DEIF, *Marine & Offshore Application Guide*, 2016.
[6] P. Kundur, *Power System Stability and Control*. McGraw-Hill, Inc., 1994.
[7] S. Roy, O. Malik, and G. Hope, "An adaptive control scheme for speed control of diesel driven power-plants," *IEEE Transactions on Energy Conversion*, vol. 6, DOI 10.1109/60.103632, no. 4, pp. 605–611, 1991.
[8] L. Guzzella and A. Amstutz, "Control of diesel engines," *IEEE Control Systems Magazine*, vol. 18, DOI 10.1109/37.722253, no. 5, pp. 53–71, 1998.
[9] K. B. Goh, S. K. Spurgeon, and N. Barrie Jones, "Higher-order sliding mode control of a diesel generator set," in *Institution of Mechanical Engineers. Part I: Journal of Systems and Control Engineering*, vol. 217, DOI 10.1243/095965103765832894, no. 3, pp. 229–241, 2003.
[10] D. McGowan, D. Morrow, and M. McArdle, "A digital PID speed controller for a diesel generating set," in *IEEE Power Engineering Society General Meeting*, vol. 3, DOI 10.1109/PES.2003.1267371, pp. 1472–1477, 2003.
[11] D. McGowan, D. Morrow, and B. Fox, "Integrated governor control for a diesel-generating set," *IEEE Transactions on Energy Conversion*, vol. 21, DOI 10.1109/TEC.2006.874247, no. 2, pp. 476–483, 2006.
[12] R. J. Best, D. J. Morrow, D. J. McGowan, and P. A. Crossley, "Synchronous islanded operation of a diesel generator," *IEEE Transactions on Power Systems*, vol. 22, DOI 10.1109/TPWRS.2007.907449, no. 4, pp. 2170–2176, 2007.
[13] D. McGowan, D. Morrow, and B. Fox, "Multiple input governor control for a diesel generating set," *IEEE Transactions on Energy Conversion*, vol. 23, DOI 10.1109/TEC.2008.918623, no. 3, pp. 851–859, 2008.
[14] A. M. Kassem and A. M. Yousef, "Robust control of an isolated hybrid wind-diesel power system using Linear Quadratic Gaussian approach," *International Journal of Electrical Power and Energy Systems*, vol. 33, DOI 10.1016/j.ijepes.2011.01.028, pp. 1092–1100, 2011.
[15] J. Mamboundou and N. Langlois, "Application of indirect adaptive model predictive control supervised by fuzzy logic to a diesel generator," in *IEEE International Conference on Control and Automation (ICCA)*, DOI 10.1109/ICCA.2011.6138065, pp. 1037–1043, 2011.
[16] G. Zhang, "Marine diesel-generator excitation controller based on adaptive on-line GA tuning PID," in *Chinese Control Conference (CCC)*, pp. 3868–3871, 2011.
[17] A. Cooper, D. McGowan, D. Morrow, and K. Chambers, "Temperature-dependant voltage regulator operation for optimal load acceptance of a diesel generator," *IET Electric Power Applications*, vol. 6, DOI 10.1049/iet-epa.2011.0218, no. 8, pp. 553–560, 2012.
[18] M. Tuffaha and J. T. Gravdahl, "Modeling and Control of a Marine Diesel Engine driving a Synchronous machine and a Propeller," in *IEEE Conference on Control Applications (CCA)*, pp. 897–904, 2014.
[19] M. Guermouche, S. Ali, and N. Langlois, "Sliding Mode Control for Diesel Generator via Disturbance Observer," *Mediterranean Conference on Control and Automation (MED)*, DOI 10.1109/MED.2015.7158795, pp. 487–494, 2015.
[20] H. Hilal, M. Oktaufik, A. Prastawa, B. Prasetyo, and R. Hutahaean, "Smart diesel generator to compensate on-grid PV fluctuation: A case study in Sumba Island Indonesia," in *Conference on Power Engineering and Renewable Energy (ICPERE)*, DOI 10.1109/ICPERE.2016.7904847, pp. 33–37, 2016.
[21] T. Broomhead, C. Manzie, P. Hield, R. Shekhar, and M. Brear, "Economic model predictive control and applications for diesel genera-

tors," *IEEE Transactions on Control Systems Technology*, vol. 25, DOI 10.1109/TCST.2016.2574758, no. 2, pp. 388–400, 2017.

[22] J. Knudsen, J. Bendtsen, P. Andersen, K. Madsen, and C. Sterregaard, "Control-Oriented First Principles-Based Model of a Diesel Generator," in *European Control Conference*, DOI 10.1109/ECC.2016.7810305, pp. 321–327, 2016.

[23] J. Knudsen, J. Bendtsen, P. Andersen, and K. Madsen, "Self-Tuning Linear Quadratic Supervisory Regulation of a Diesel Generator using Large-Signal State Estimation," in *Australian Control Conference*, DOI 10.1109/AUCC.2016.7867928, pp. 32–37, 2016.

[24] R. H. Park, "Two-Reaction Theory of Synchronous Machines - Generalized Method of Analysis - Part I," *Journal of the American Institute of Electrical Engineers*, vol. 48, DOI 10.1109/T-AIEE.1929.5055275, no. 3, pp. 716–727, 1929.

[25] MathWorks, "Simscape Power Systems," 2017. [Online]. Available: https://se.mathworks.com/products/simpower.html

[26] S. E. Lyshevski, *Electromechanical Systems, Electric Machines, and Applied Mechatronics*. CRC Press, 1999.

[27] IEEE Power Engineering Society, "IEEE Guide: Test Procedures for Synchronous Machines," *IEEE Std 115-1983 (Revision of IEEE Std 115-1965)*, DOI 10.1109/IEEESTD.1983.86121, p. 87, 1983.

[28] IEEE Power Engineering Society, "IEEE Guide for Test Procedures for Synchronous Machines," *IEEE Std 115-2009 (Revision of IEEE Std 115-1995)*, DOI 10.1109/IEEESTD.2010.5464495, p. 207, 2010.

[29] Mecc Alte, *Generator Type ECO 32-3S/4*. Datasheet, 2012.

[30] Leroy-Somer, *Low Voltage Alternators - 4 pole*. Datasheet, 2015.

[31] D. G. Luenberger, "Observers for Multivariable Systems," *IEEE Transactions on Automatic Control*, vol. 11, DOI 10.1109/TAC.1966.1098323, no. 2, pp. 190–197, 1966.

[32] B. D. O. Anderson and J. B. Moore, *Optimal Control: Linear Quadratic Methods*. Prentice-Hall, Inc., 1989.

[33] S. Skogestad and I. Postlethwaite, *Multivariable Feedback Control*. John Wiley & Sons, Inc., 1996.

[34] J. Hespanha and A. Morse, "Stability of Switched Systems with Average Dwell-Time," in *Proceedings of the 38th IEEE Conference on Decision and Control (Cat. No.99CH36304)*, vol. 3, DOI 10.1109/CDC.1999.831330, no. December, pp. 2655–2660, 1999.

[35] DSPACE, "DS1103," 2015. [Online]. Available: https://www.dspace.com/en/inc/home/support/pli/elas/elads1103.cfm

[36] J. Kautsky, N. K. Nichols, and P. Van Dooren, "Robust Pole Assignment in Linear State Feedback," *International Journal of Control*, vol. 41, DOI 10.1080/0020718508961188, no. 5, pp. 1129–1155, 1985.

Jesper Knudsen was born in Aalborg, Denmark in 1989. He received the M.Sc. degree from the Section for Automation and Control, Department of Electronic Systems, Aalborg University, Aalborg, Denmark in 2014. From 2015 to 2017 he has been an Industrial Ph.D. Fellow in the Section for Automation and Control in collaboration with DEIF; submitting his Ph.D. thesis in December, 2017.

He has been a Control Engineer in the R&D Technology department of DEIF, Skive, Denmark since 2018. As part of his M.Sc., he was a Visiting Student with Massachusetts Institute of Technology, Cambridge, MA, USA from 2013 to 2014. In 2016, he was a Visiting Researcher with The University of Sheffield, Sheffield, UK.

Mr. Knudsen was a recipient of the Bikuben–Denmark-America Foundation Fellowship in 2013 for his stay with Massachusetts Institute of Technology.

Jan D. Bendtsen (M'11) was born in Denmark in 1972. He received the M.Sc. and Ph.D. degrees from the Department of Control Engineering, Aalborg University, Aalborg, Denmark in 1996 and 1999, respectively.

He has been an Associate Professor with the Department of Electronic Systems, Aalborg University, since 2003. In 2005, he was a Visiting Researcher with Australian National University, Canberra, ACT, Australia. Since 2006, he has been involved in the management of several national and international research projects, and organizing international conferences. From 2012 to 2013, he was a Visiting Researcher with the University of California at San Diego, La Jolla, CA, USA. His current research interests include adaptive control of nonlinear systems, closed loop system identification, control of distribution systems, and infinite-dimensional systems.

Dr. Bendtsen was a co-recipient of the Best Technical Paper Award at the American Institute of Aeronautics and Astronautics Guidance, Navigation, and Control Conference in 2009.

Palle Andersen (M'13) was born in Vesthimmerland, Denmark in 1951. He received the B.Sc.EE (1974) and the Ph.D. degree (1977) from Aalborg University, Aalborg, Denmark.

He was with the municipality in Randers from 1978 to 1986 with responsibility for automatic control of water supply, district heating and power production and distribution. Since 1986, he has been with Aalborg University; from 1991 as Associate Professor working with control engineering including optimal, robust and model predictive control. Research interests include modeling and control of energy systems, power plant boilers, marine boilers, wave energy conversion, district heating and waste water systems.

Dr. Andersen has received the IFAC Control Engineering Practice Prize Paper Award for a paper on optimizing control of power plant boilers.

Kjeld K. Madsen was born in Herning, Denmark in 1971. He received his B.Sc.EE in Process control from Herning Institute of Business And Technology, Herning, Denmark in 2000.

He has been with DEIF, Skive, Denmark, since 2000; from 2016 as a Senior Engineer in the R&D Technology department. Since 2014 he has been involved in research activities within the fields of control and electric power system protection.

Claes H. Sterregaard was born in Odense, Denmark in 1977. He received his M.Sc.EE in Electro Mechanical System Design from Aalborg University, Aalborg, Denmark in 2002.

He has been with DEIF, Skive, Denmark since 2003; from 2003 to 2009 as a Software Designer. From 2009 to 2012 as Senior Specialist. From 2012 to 2013 as Product Manager for IPP products. From 2013 to 2016 as Product Manager for hybrid products. Since 2016 as Program Manager for Microgrids.